Out of Africa by spontaneous migration waves

Paul D. Bons[1]*, **Catherine C. Bauer**[1,2], **Hervé Bocherens**[1,2], **Tamara de Riese**[1], **Dorothée G. Drucker**[1,2], **Michael Francken**[1,2], **Lumila Menéndez**[1,3], **Alexandra Uhl**[4], **Boudewijn P. van Milligen**[5], **Christoph Wißing**[1]

1 Department of Geosciences, Eberhard Karls University Tübingen, Tübingen, Germany, 2 Senckenberg Centre for Human Evolution and Palaeoenvironment (HEP), Tübingen, Germany, 3 Departamento de Antropología, Universidad Nacional de La Plata, La Plata, Argentina, 4 Department of Anthropology, Boston University, Boston, Massachusetts, United States of America, 5 National Fusion Laboratory, CIEMAT, Madrid, Spain

* paul.bons@uni-tuebingen.de

Abstract

Hominin evolution is characterized by progressive regional differentiation, as well as migration waves, leading to anatomically modern humans that are assumed to have emerged in Africa and spread over the whole world. Why or whether Africa was the source region of modern humans and what caused their spread remains subject of ongoing debate. We present a spatially explicit, stochastic numerical model that includes ongoing mutations, demic diffusion, assortative mating and migration waves. Diffusion and assortative mating alone result in a structured population with relatively homogeneous regions bound by sharp clines. The addition of migration waves results in a power-law distribution of wave areas: for every large wave, many more small waves are expected to occur. This suggests that one or more out-of-Africa migrations would probably have been accompanied by numerous smaller migration waves across the world. The migration waves are considered "spontaneous", as the current model excludes environmental or other extrinsic factors. Large waves preferentially emanate from the central areas of large, compact inhabited areas. During the Pleistocene, Africa was the largest such area most of the time, making Africa the statistically most likely origin of anatomically modern humans, without a need to invoke additional environmental or ecological drivers.

Introduction

Hominins are generally supposed to have originated in Africa and settled most of Africa and the southern half of Eurasia in the early Pleistocene [1–5]. Fossil evidence suggests that earliest *Homo sapiens* appeared in Africa during the late Middle Pleistocene (Jebel Irhoud, Omo and Herto [6–8]). Anatomically modern humans (AMH) emerged, spread out of Africa during the Late Pleistocene and now occupy the whole world as the only Homo species [9–14]. In the intervening time, a number of Homo species, such as Neanderthals, Denisovans, *Homo erectus*, *H. heidelbergensis*, *H. ergaster*, etc. existed, developed and disappeared again [15–22]. Pleistocene human evolution is thus characterised by differentiation, speciation, migration waves and extinction events. Most authors assume that the out-of-Africa spread of AMH involved

one or more migration waves that replaced *Homo* species that existed at the time with only limited genetic admixture, such as between Neanderthals and AMH [23–24]. Many studies have addressed the timing and origin of migration waves, as well as migration paths (e.g. [13,23,25–27]). Apart from the major out-of-Africa event(s), AMH populations experienced several more migration waves within already populated areas, such as Africa [28–29] and Europe [30–31]. Considering this, it is not unlikely that more migration waves occurred in the Pleistocene, but the sparse fossil record still makes it difficult to detect any.

Assuming that migration waves did happen, the question arises what caused them, in particular in relation to the spread of AMH. Most authors favour some competitive advantage of AMH over other *Homo* species [32–34]. With climate change now central in the scientific discourse, many recent studies suggest that climate played an important role in the environmental changes making AMH more competitive than other *Homo* species, or allowing the opening of ecological corridors that triggered the dispersal of *Homo sapiens* out of Africa [35–44]. An opposite view is that AMH and Neanderthals actually had no competitive advantage over each other [45]. The argument, based on a numerical model, is that, because AMH's population was much larger than that of Neanderthals [12,46–48], AMH's were statistically more likely to reach fixation in both Africa and Europe.

Although modelling is extensively used in studies of human evolution (e.g. [49–51]), relatively few studies so far employed forward approaches on an explicit map to, for example, determine amounts of admixture, stepping stones or the most probably origin of AMH [39,45,52–55]. Kolodny and Feldman [45] used a simple "map" with only two demes to determine the chances that AMH would replace Neanderthals purely due to the larger population of AMH in Africa compared to Neanderthals in Europe. The SPLATCHE2 simulations [55] and the similar model by Eriksson et al. [39] assumed *a priori* that AMH have some advantage and explored the advance of AMH in relation to climate factors. These various models have in common that the species (AMH) and its competitive advantage are predefined in the parameters of the model.

Here we present a basic numerical model to simulate the spatial and temporal differentiation/speciation and the emergence, frequency and patterns of migration waves. The model is not restricted to any particular species, but is applied here to human evolution, because there is probably no other species than AMH whose evolutionary origins have attracted so much general and scientific interest. Contrary to the above-mentioned models, no human species are defined *a priori*. The only aim is to explore the statistics of patterns, without claiming or attempting to simulate the actual emergence and spread of AMH, which would only be one of an infinite number of realisations of the stochastic model. Although a range of environmental factors have been invoked to explain various aspects of human evolution, we expressly do not include these in the models presented here. The premise here is that neutral evolutionary processes already lead to complex and emergent behaviour that resulted in human evolution patterns, including migration waves. The aim is thus to provide a null hypothesis against which additional environmental factors and influences can be further tested.

Methods

The model is based on a regular 2-dimensional grid of demes, each a square area with a number of individuals. The genome (*G*; see Table 1 for list of symbols) of a deme is defined by a single string of *N* binary genes, with two alleles, either zero or one (similar to e.g. [56–57]). This genome is the single dominant or representative genome for the population of a deme. The temporal and spatial evolution of genomes is modelled in discrete time steps of length Δt in which mutations take place and genes are transferred between neighbouring demes. The

Table 1. List of symbols and abbreviations in order of appearance in text.

Symbol	Definition/description
G	The genome of a single deme, expressed as a binary string of zeros and ones
N	Number of genes in a genome. Typically at least several hundreds.
$t, \Delta t$	Time and duration of a numerical time step
M	Number of mutations occurring in the whole model per time step. Set to 4 per time step.
m	Chance, per time step, that a mutation occurs in a particular deme
A	Total number of populated demes in model
N_D	Number of individuals that populate one deme (Eqs 3 and 4)
T	Number of generations per time step (Eq 3)
S	Linear dimension of a deme (Eq 4)
m_0	Mutation rate of a single individual
s	Competitive advantage
D	Parameter defining the chance, per time step, that an allele jumps from one deme to a neighbour (Eq 1).
α	Assortative mating factor (Eq 1). Set to either 0 or 0.05.
ΔG	Number of genes that have different alleles in two neighbouring demes (Eq 1)
D_0	Reference diffusion coefficient (equals D when $\alpha = 0$). Always set to unity here (Eqs 1 and 7).
p	Advantage factor, defining the rate at which an allele "1" spreads at the cost of its counterpart "0" (Eqs 2,4,6 and 7). Varied from 0.0125 to 0.05 in Fig 1; set to 0.05 in other figures.
F	"Fitness" of a genome: the sum of all alleles in one deme's genome (Eq 2).
ΔF	"Fitness" difference between two neighbouring demes (Eq 2).
ρ	Population density in number of individuals per km^2 (Eq 4)
A_{mut}	Area in number of demes occupied by a mutation (a gene with the allele "1" instead of "0") (Eq 5)
r_{eq}	Radius of a circle with the same area as that occupied by a mutation (A_{mut}) (Eqs 5 and 6)
v	Spreading velocity of a mutation (Eq 5)
L_{if}	Length of the perimeter of an area occupied by a mutation (Eq 6)
P_{fix}	Mean chance of a mutation to reach fixation in whole model
N_{fix}	Number of mutation that have reached fixation in whole model
t_{fix}	Mean time for a mutation to reach fixation in whole model
f	Frequency of the occurrence of sweeps of a certain area (Eq 8)
A_n	Normalised area of a sweep (number of swept demes/total number of populated demes in model) (Eq 8)
q	Exponent in power-law distribution of sweep areas (Eq 8)

https://doi.org/10.1371/journal.pone.0201998.t001

distribution of genomes is visualised in RGB colour maps in which each deme is one pixel. Red is proportional to the number of ones in the deme's genome, blue proportional to the number of genes identical to G = {10101010, etc.} and green proportional to the number of genes identical to G = {00110011, etc.}. Colours are stretched to maximise the colour range.

Mutations

Mutations are carried out at the start of each time step (See S2 Fig for the workflow). For each mutation, a deme is first randomly picked. Next, a random gene that has allele "0" everywhere in the model is chosen. This gene will mutate by changing its allele from "0" to "1" in the deme. This procedure is repeated M times (the mutation rate) per time step. The mutation chance (m) per time step for one single deme is $m = M/A$, with A the area of the model. m is the chance that one mutation emanating from a single individual reaches fixation in the whole population (of size N_D) of a single deme in a time step of T generations. m thus depends on T, N_D (itself the product of population density ρ and area S^2 of a deme) and the intrinsic mutation rate m_0 of one individual per generation. The number of mutations that occur in one deme per generation is proportional to $N_D \cdot m$. However, the chance that a mutation reaches fixation

within the population is roughly inversely proportional to N_D for $s \approx 0$, with s the competitive advantage [58]. It follows that the rate of successful mutations within the deme is proportional to m_0, and is not dependent on the population size of the deme. The model, however, uses time steps T of more than one generation. It will be shown below that $T \propto N_D$, and hence, $m \propto m_0 \cdot N_D$.

We use the term "active mutations" for those mutations that have not reached fixation, i.e. they occupy at least one, but not every deme in the map of all demes. Once a mutation has reached fixation by occupying every deme in the model it no longer plays an active role. The timing of fixation of a mutation is recorded, as well as the location of origin of the mutation.

Allele exchange between neighbours

A mutation step is followed by one round of interbreeding in which single alleles may be transferred between neighbouring demes (here using a Von Neumann direct neighbourhood scheme). All demes are considered on average once in a random order for transfer between a deme (deme a) and a randomly selected direct neighbour (deme b). Each pair is thus treated every two steps on average. The chance that a transfer between neighbouring deme is considered in one time step is defined by the parameter D. It can be regarded as a general diffusion parameter: the chance, per time step, that an allele jumps from one deme to a neighbour by following a random Brownian movement [58–61]. Assortative mating [62] is included in a way similar to the model of Barton and Riel-Salvatore [54]. With assortative mating, similar individuals are more likely to mate than different ones. This is implemented with the "assortative mating factor" (α), which reduces D as a function of ΔG, which is the number of genes that have different alleles in the two neighbouring demes under consideration:

$$D = D_0(1 - \alpha \Delta G), \text{ with } \Delta G = \sum |G_{(a)} - G_{(b)}| \tag{1}$$

D_0 is the reference diffusion parameter, equal to D for the case that $\alpha = 0$. It is first decided with a random-number generator whether a gene transfer will take place or not, according to (Eq 1). If this is to happen, all genes in the list are considered for allele transfer. The chance $P(a \rightarrow b)$ that an allele of the genome of deme a is copied to deme b is calculated with:

$$P(a \rightarrow b) = 0.5 + p\Delta F_{a,b}, \text{ with } \Delta F_{a,b} = \sum G_{(a)} - \sum G_{(b)} \text{ and } P(b \rightarrow a) = 1 - P(a \rightarrow b) \tag{2}$$

$\Delta F_{a,b}$ is the difference in number of mutations (ones) between the two demes. The chance that a deme passes on its mutations to a neighbour is thus determined by the overall number of mutations relative to that neighbour ($\Delta F_{a,b}$) and the advantage factor p that defines the competitive advantage of these mutations (assumed the same for all mutations). In this paper we define the sum of all genes ($F = \Sigma(G)$) as the "fitness" of a deme. This is because the number of advantageous genes (F), multiplied by the advantage factor (p) determines the chance that genes are passed on to offspring. When $p = 0$, mutations are neutral and there is no preferential transfer of alleles and we have purely random spreading of zeros and ones, but, on average, no change in their frequency. A positive value of p leads to fitter demes to pass on their alleles to their neighbours. Note that the transfer chance of a single allele does not only depend on its own value, but on that of the whole genome. This can potentially lead to less competitive zeros replacing more competitive ones.

To estimate the duration of one time step, we can consider the population of the two neighbouring demes as one during the transfer. Of interest is the case where the mutation only occurs in one of the two demes, i.e. when it is carried by 50% of the combined population. The time step T (in number of generations) is thus the time it takes for a mutation to reach fixation

by genetic drift in the combined population with a chance of 0.5+p or extinction with a chance of 0.5-p. Using a basic Monte Carlo model for populations of up to a few hundred individuals, we find for the time step T (Equation C in S1 File):

$$T \approx \gamma \frac{\rho S^2}{D_0} = \gamma \frac{N_D}{D_0} \tag{3}$$

Here, S is the size of a deme and ρ the population density. (Eq 3) only holds for weakly competitive mutations ($s \ll 1$), small values of p, and no variation in population density between demes. The factor p is related to s, the competitive advantage of the mutation [58–61,63] (Equation B in S1 File):

$$p \approx 0.29 \cdot \rho S^2 \leftrightarrow s \approx 3.4 \frac{p}{\rho S^2} = 3.4 \frac{p}{N_D} \tag{4}$$

At a deme size of $S = 50$ km and a population density of 0.01 individuals/km^2, T is about 175 generations ($\approx$4000 years at 25 years/generation) for $D_0 = 1$ as used throughout this paper. Using $p = 0.05$ results in a competitive advantage of $s \approx 0.7\%$.

Spreading of mutations

A single mutation in a field of demes without any other mutations has a chance of 0.5-p to disappear the first time an interbreeding event is considered with one of its neighbours. The initial survival rate is thus a function of p. The low initial survival rate is due to two factors. The first is a numerical effect that the width of diffusional front is less than can be resolved at the scale of the demes. The second is related to genetic drift [64–65], where the effective population (cluster of demes around the new mutation) is small and therefore the chance of survival smaller than when the mutation has spread over a large area.

Once a mutation has survived this initial nucleation phase by spreading over sufficient demes, the area occupied by the deme increases linearly with time. The expansion front is not sharp, but diffuse, in accordance with the diffusion-reaction model of [59]. The width of the diffusional front decreases with increasing p (Fig 1A–1C) as the advantage factor becomes more important relative to the diffusional spreading. After the initial nucleation phase, the area (A_{mut}) occupied by the single mutation increases linearly with the square of time. We define the velocity (v, in deme size per time step) of the expanding front as the rate of increase in radius (r_{eq}) of an equivalent circle with area A_{mut}:

$$v = \frac{dr_{eq}}{dt} = \frac{d(\sqrt{A_{mut}/\pi})}{dt} \tag{5}$$

The spreading velocity ($v_{(p)}$) as a function of p is determined from 2500 simulations of an expanding mutation after a stable diffusive front has been established ($50 < r_{eq} < 150$ demes). $v_{(p)}$ is determined by the chance (proportional to p) that the mutation is copied to a deme without that mutations and the length (L_{if}) of the interface between demes with and without that mutation. L_{if} is much larger than the circumference ($2\pi r_{eq}$) of the equivalent circle in case of a diffusive front. $L_{if}/2\pi r$ thus decreases with p and can be approximated with a power law (using a least-squares best fit, with $r^2 = 0.99565$; Fig 1D):

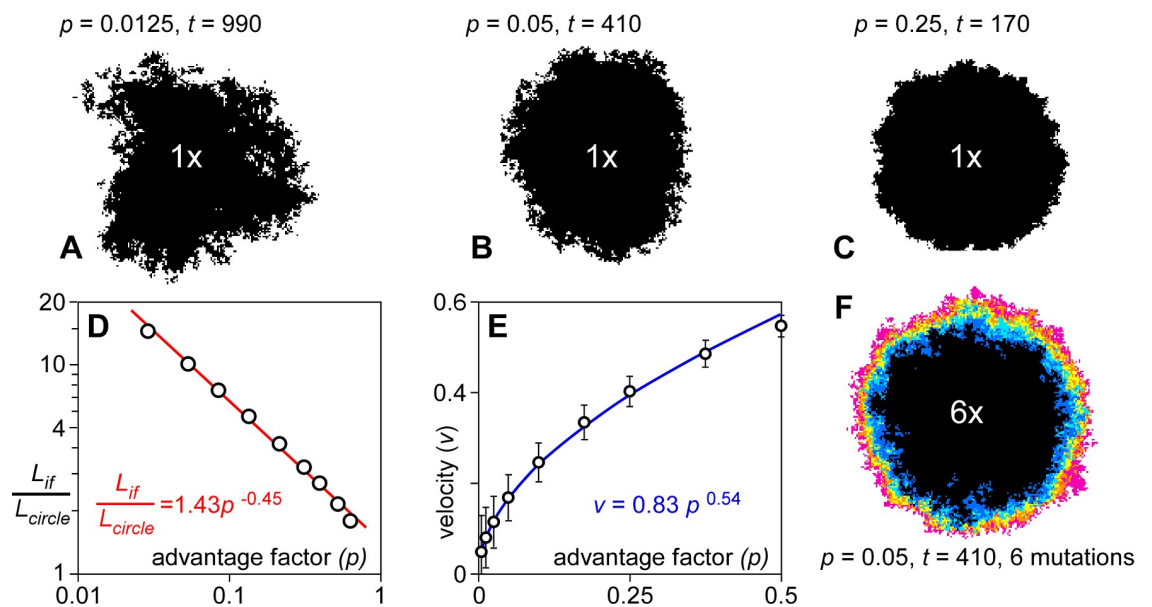$$\frac{L_{if}}{2\pi r_{eq}} \approx 1.43 \cdot p^{-0.45} \tag{6}$$

Fig 1. Spreading rates of mutations. Distribution of a single mutation originating from the centre of a circular model ($R = 100$ demes) at the stage where the effective radius of the area occupied by the mutation is 60 demes. **A.** $p = 0.0125$ at $t = 990$. **B.** $p = 0.025$ at $t = 720$. **C.** $p = 0.05$ at $t = 410$. The effect of increasing p is an increase in spreading rate and a sharpening of the spreading front. **D.** Interface length divided by effective circle circumference versus drift factor in a double-log plot. Data approximately follow a power law. **E.** As a result, spreading velocity versus advantage factor also shows a power-law relationship. **F.** Distribution of six mutations seeded at the centre of the model ($R = 100$ demes) at $t = 0$. Colours show number of mutations on a deme from one (pink) to six (black).

As a result, $v_{(p)}$ (in deme/step) is approximately a power-law function of p ($r^2 = 0.9993$; Fig 1E):

$$v_{(p)} = D_0 \cdot 0.83 \pm 0.02 \cdot p^{0.54} \qquad (7)$$

The exponent is slightly larger than 0.5 due to the fact that the spreading front becomes less fuzzy with increasing p. This means that demes at the front have fewer neighbours without the mutation when p is large than when it is small.

The initial spreading velocity is higher when multiple mutations are placed in the centre of the model (Fig 1F). This is expected, because $\Delta F > 1$ in (Eq 2). However, the steady-state velocity of these mutations is the same when the diffusion front is wide enough (low p). The explanation is that demes within this diffusive front mostly only have a low ΔF with their direct neighbours and thus spread as fast as a single mutation. This implies that gene surfing due to high ΔF is not effective during steady-state spreading of an ensemble of mutations. However, spreading rate increases when fitness gradients or clines are high due to a high mutation rate, or when two different populations, with high ΔF, would suddenly come into contact.

Replacement events

Full genome transfers or replacement events are considered after the interbreeding step. Again, all demes and one random direct neighbour are considered in a random order. A full genome replacement is carried out if the absolute fitness difference $|\Delta F|$ is equal or greater than a set critical fitness difference ΔF_{crit}. In that case, the full genome of the fittest deme is copied to that of its neighbour. After one round where all demes and one random neighbour are considered once for a replacement, the replacements may have led to new pairs that exceed ΔF_{crit}. The

routine is therefore repeated until $\Delta F < \Delta F_{crit}$ everywhere in the model. When Δt is small, this semi-instantaneous spreading would be relatively fast (up to the order of a km/yr, depending on the size of demes). However, we use this scheme here to be able to track individual replacement "avalanches" within one time step. Contiguous areas that experienced a full genome replacement are termed "sweeps" here. The time and area of each sweep (A_{sw}) is recorded at the end of each time step, as well as a map of all demes that experienced a genome replacement sweep.

Aims

The aim of this paper is to test the main types of evolutionary patterns that result from different combinations of diffusive spreading with competitive advantageous mutations, assortative mating and replacement waves. It is not our intention to systematically investigate and quantify the effect of each of the parameters. We therefore only evaluate four representative cases (Table 2), using a reference model with 3 square inhabited areas, connected by narrow

Table 2. Summary of the main effects of assortative mating and migration sweeps.

	No assortative mating ($\alpha = 0$)	With assortative mating ($\alpha > 0$)
No migration sweeps (ΔF_{crit} not reached)	**Fig 2A.** Spreading of mutations leads to gradual gradients in genetic signature (ΔG) and fitness (ΔF). Gradients are a function of the mutation rate (M) in relation to the demic diffusion rate (D_0) in combination with the advantage factor (p), a function of the competitive advantage (s) of mutations. Fitness maxima (largest number of mutations) are found in the centre of large compact populated areas. Variation develops by isolation-by-distance, but no distinct subspecies develop.	**Fig 2B.** Spreading of mutations leads to gradual gradients in genetic signature (ΔG) and fitness (ΔF). With increasing ΔG, "nation-like" regions develop with sharp gradients at their boundaries. Genomes within regions are relatively homogeneous as mutations within a region can reach fixation within the whole region. Genomes within regions evolve relatively slowly as mutations do not, or only rarely cross regional boundaries. Size of regions depends on mutation rate (M), relative to the diffusion rate (D_0) and advantage factor (p), and the assortative mating factor (α). Pattern is close to spatially static multi-regional or structured populations with multiple split events in populations that develop distinct genetic signatures.
	Gradients in genetic signature (ΔG) and, hence, in fitness (ΔF) increase until they reach the threshold (ΔF_{crit}) for the initiation of migration sweeps. Migration sweeps follow a power law function for their frequency as a function of swept area (Eq 8), with many smaller sweeps for each large one. The very largest sweeps are more common than the power-law predicts ("dragon kings").	
With migration sweeps (ΔF_{crit} regularly reached)	**Figs 3 and 8A.** Migration sweeps bring originally spatially isolated genomic signatures in contact to allow for admixture in the absence of assortative mating. Admixture results in rapidly increasing genetic signature gradients that initiate new migration sweeps. Periods of gradual differentiation by isolation-by-distance are interspersed by shorter "bursts" of migration sweeps and a complete reorganisation of the genetic signature, resulting in a relatively homogeneous genetic signature in the whole populated area at the end of one cycle. Consistent with a punctuated equilibrium model with regular cycles.	**Figs 4 and 8B.** The amount of structuring of the population in distinct regional genetic types depends on the importance of assortative mating (α) relative to the threshold for the initiation of migration sweeps (ΔF_{crit}). These sweeps bring originally spatially isolated genomic signatures in contact with each other, but assortative mating inhibits/reduces admixture between these. Assortative mating therefore reduces the clustering in time of migration sweeps and reduces admixture. The latter allows the preservation of older genetic signatures, preferentially in the centre of large populated areas (e.g. Africa) that experience fewer migration sweeps. Consistent with multi-regionalism or structured populations, preservation of archaic signatures, as well the punctuated equilibrium model with the occurrence of both large and many small migration sweeps.

isthmuses. The areas or "continents" are 100x100, 50x50, and 25x25 demes in size. In each individual simulation presented below we keep all parameters constant in space and time. This implies that any environmental factors that could affect the competitive advantage of individual mutations, their spreading rate, and the population density do not change spatially or in time. This serves the aim of this paper to investigate patterns that develop in the complete absence of any environmental or other external influences, with the exception of coastlines and mountain ranges that act as barriers. We consider this as a fundamental preliminary step in order to further discuss diversification processes during human evolution.

Results and discussion

Diffusion effect

We first consider the case (Fig 2A) without genome replacements ($\Delta F_{crit} = \infty$) or assortative mating ($\alpha = 0$). The mutation rate M is set to four mutations per time step and p is 0.05. Individual mutations spread leading to increasing variation in genomes within the model. This is comparable to the geographic differentiation through isolation-by-distance as proposed for the reticulate or multiregional evolution model [66–67] or the recent assimilation model [68–69].
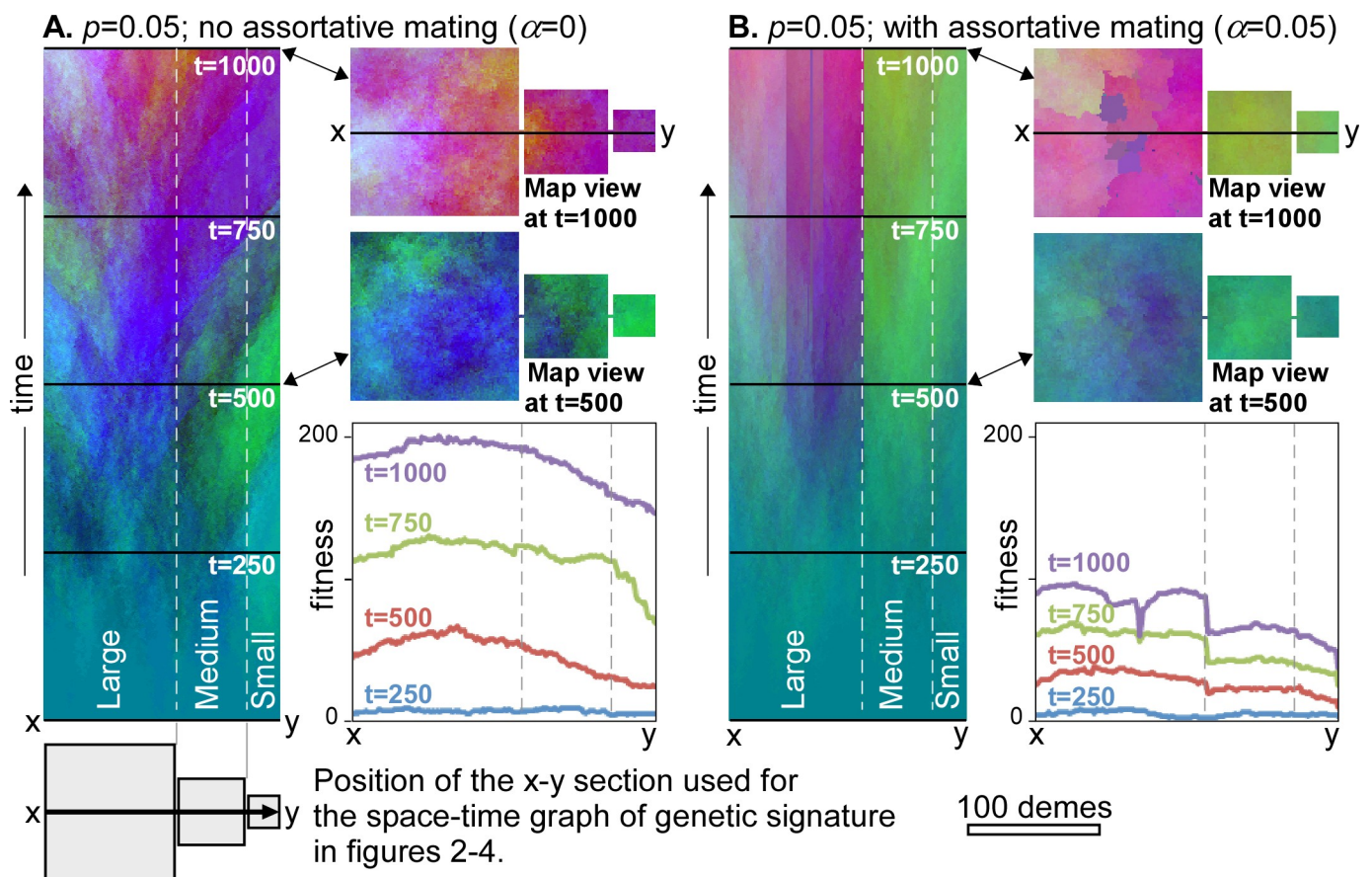

Fig 2. Time evolution of genome signatures over 1000 steps. Left column shows the genome signature along the east-west x-y section through the centre of the three continents as a function of time along the vertical axis. Right column shows map views of genetic variations at stages 500 and 1000. Colours qualitatively represent variations in genome, with the red tones proportional to "fitness". Graphs show the fitness profiles along the x-y section at four time steps. **A.** In case of diffusion only, genetic signatures tend to emanate from the centre of the occupied areas and spread out towards the margins. **B.** When assortative mating is added, internally relative homogeneous "nation" regions with sharp boundaries develop from about $t = 500$ steps. As these boundaries inhibit spreading of mutations, overall fitness increases more slowly than without assortative mating.

https://doi.org/10.1371/journal.pone.0201998.g002

Demes in the centre of the model are on average nearer to the origins of mutations than are demes on the periphery. Fitness therefore increases faster in the centre than the periphery, as can be seen in the fitness profile across the three "continents" (Fig 2A). After steady outward fitness gradients are established at about $t = 250$, genetic signatures migrate outwards, down the gradients. Signatures in the periphery are thus regularly overprinted by those coming from the centre.

The effect of assortative mating

The effect of the assortative mating factor (α) is to reduce the rate of gene exchange when the genomes of neighbouring demes are different. Fig 2B shows the effect of assortative mating in the same model as Fig 2A, but with α set to 0.05. This means decreasing genetic exchange up to $\Delta G = 20$, where exchange is reduced to zero. With initially low variations in genetic signature, the effect in the beginning is only to slow down differentiation. At about $t = 500$, first neighbouring demes cease exchanging alleles, which allows their ΔG to increase further. This finally leads to homogeneous regions, bounded by fixed, sharp borders. In Fig 2B these are visible as persistent, sharp changes in colour. New mutations cannot escape these "nations". Because the fixation time within a "nation" is smaller than for the whole model, these mutations can now spread significantly before more mutations occur, thus keeping ΔG and ΔF low within a "nation", while F for each "nation" keeps rising steadily. A large area, high mutation rate and low spreading rate (low D_0 and p) all favour high values of both ΔF and ΔG (with $\Delta G \geq \Delta F$). When these values remain too low, incipient borders shift and weaken again, which inhibits the establishment of permanent borders. This effect is visible in the medium and small "continents" that now behave as a closed system with highest fitness in the centre, but no internal "nation" borders. The development of "nations" or a structured population [70] results in a breakdown of the positive relationship (Fig 2A) between genetic signature and distance between points or isolation by distance [71]. This leads to a relative isolation of demes, which is strengthened through time.

Effect of replacement sweeps

The effect of replacement is again illustrated with the three-continent model (Fig 3), using the same $p = 0.05$ and M of four mutations per time step as before. ΔF_{crit} is set at 10, so the genome of a deme is fully replaced by that of its neighbour if that neighbour has at least 10 mutations more.

In the absence of assortative mating ($\alpha = 0$), fitness increases steadily, especially in the centre of the model, until gradients exceeding ΔF_{crit} are reached (at $t = 274$ in Fig 3A). This typically happens somewhere between the centre and the margin. This is because, although fitness is highest in the centre, gradients are generally low here. Gradients are highest near the margins, where fitness is lower than in the centre. As a result, replacements first sweep the margins of the model ($t = 274$), skirting the high-fitness centre (for example at $t = 296$). Demes in the swept area with a single genome subsequently exchange alleles with the unswept demes, which rapidly leads to genomes with enhanced fitness again, and, hence, new sweeps ($t = 299$). A rapid succession of admixture and replacement sweeps leads to homogenisation of the genome over the whole area. Although the new global genome is closest to that of the centre of the model, there are significant changes by admixture during the various successive sweeps.

After homogenisation of the genome, it takes some time for gradients to develop again to initiate a new cycle of replacement sweeps. This leads to a regular cycle of 200–300 time steps of differentiation without any sweeps, followed by a rapid succession of many small and a few large sweeps that sweep almost the whole model area (Fig 3A). This pattern is in line with the
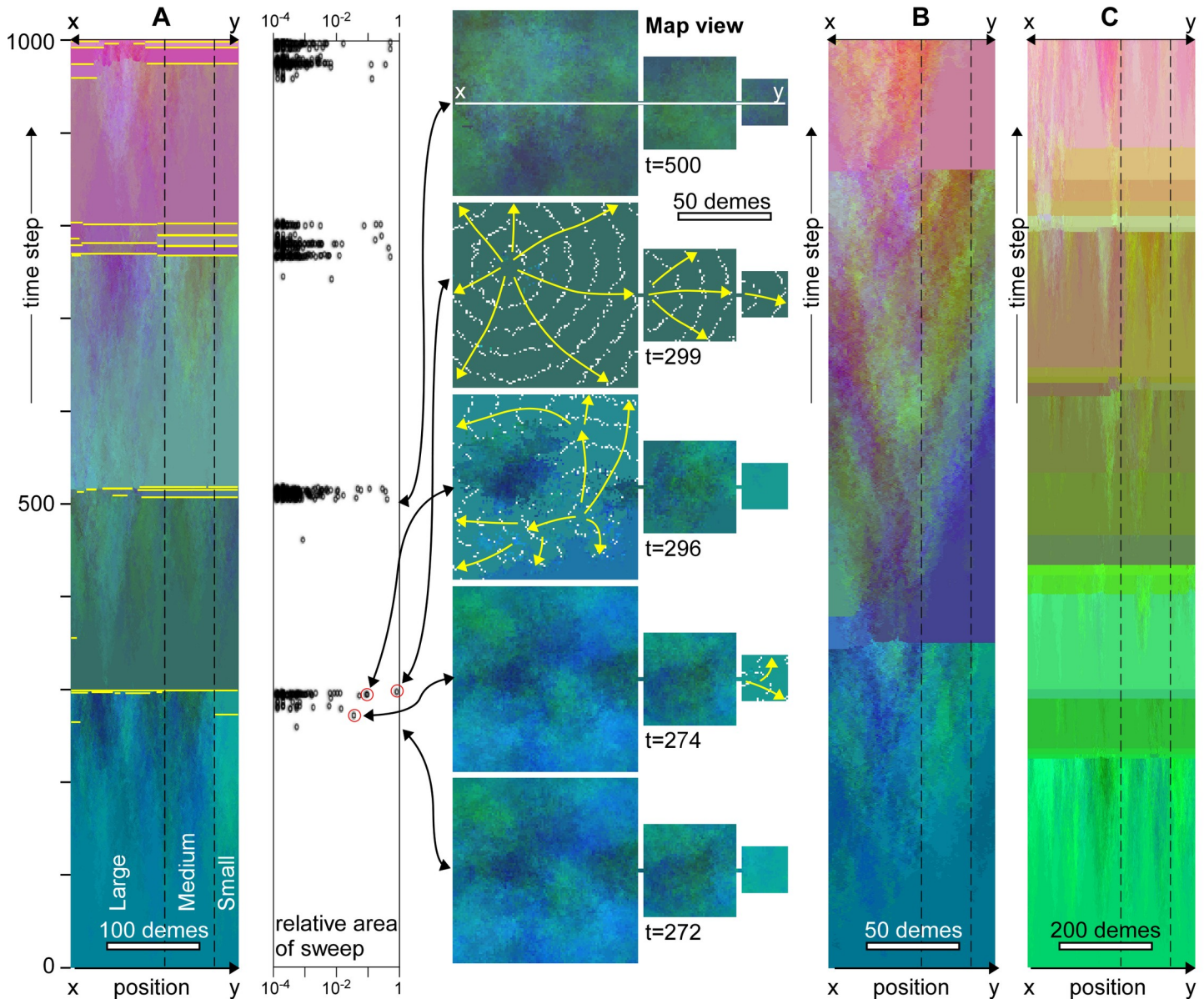
Fig 3. Evolution of genetic signatures in case of replacement sweeps in the absence of assortative mating. A. Temporal evolution along the line x-y through the centre of the model (see Fig 2). Sharp changes in colour indicate replacement sweeps. The main ones are highlighted in yellow. Graph shows the area (A_n, relative to total area) of individual sweeps as a function of time. Replacement sweeps are strongly clustered in time. Map views show the genetic distribution at five selected points in time. Direction and extent of selected sweeps at t = 274, 296 and 299 are shown by yellow arrows and white lines that trace the front at regular time intervals, respectively. These sweep events are highlighted with red circles in the A_n versus time graph. Doubling (**B**) or halving (**C**) the deme size (S) roughly doubles or halves, respectively, the average time interval between clusters of replacement sweeps, but not the general pattern.

https://doi.org/10.1371/journal.pone.0201998.g003

punctuated-equilibrium model [72–74]. Reducing the resolution by a factor two, while keeping all other parameters the same, implies reducing the population density and the frequency of mutations in the model by a factor four. Gradients now increase at a lower rate and the duration of a full cycle is roughly doubled (Fig 3B). Doubling the resolution has the opposite effect and leads to a reduction of the cycle time (Fig 3C). Independent of resolution, admixture results in several large sweeps that together reset the genomes in the whole area.

Adding assortative mating ($\alpha = 0.05$) to the previous simulation significantly changes the evolution of the model (Fig 4A). After the initial differentiation period, first sweeps occur and, again, mostly sweep the margins. Contrary to the previous case where $\alpha = 0$, the sweeping genome is now unlikely to interbreed with fit demes at the edge of the swept area owing to their large ΔG. New sweeps are thus not immediately triggered for lack of admixture, and sweeps are less clustered in time. Demes in the centre are rarely or even never swept, providing
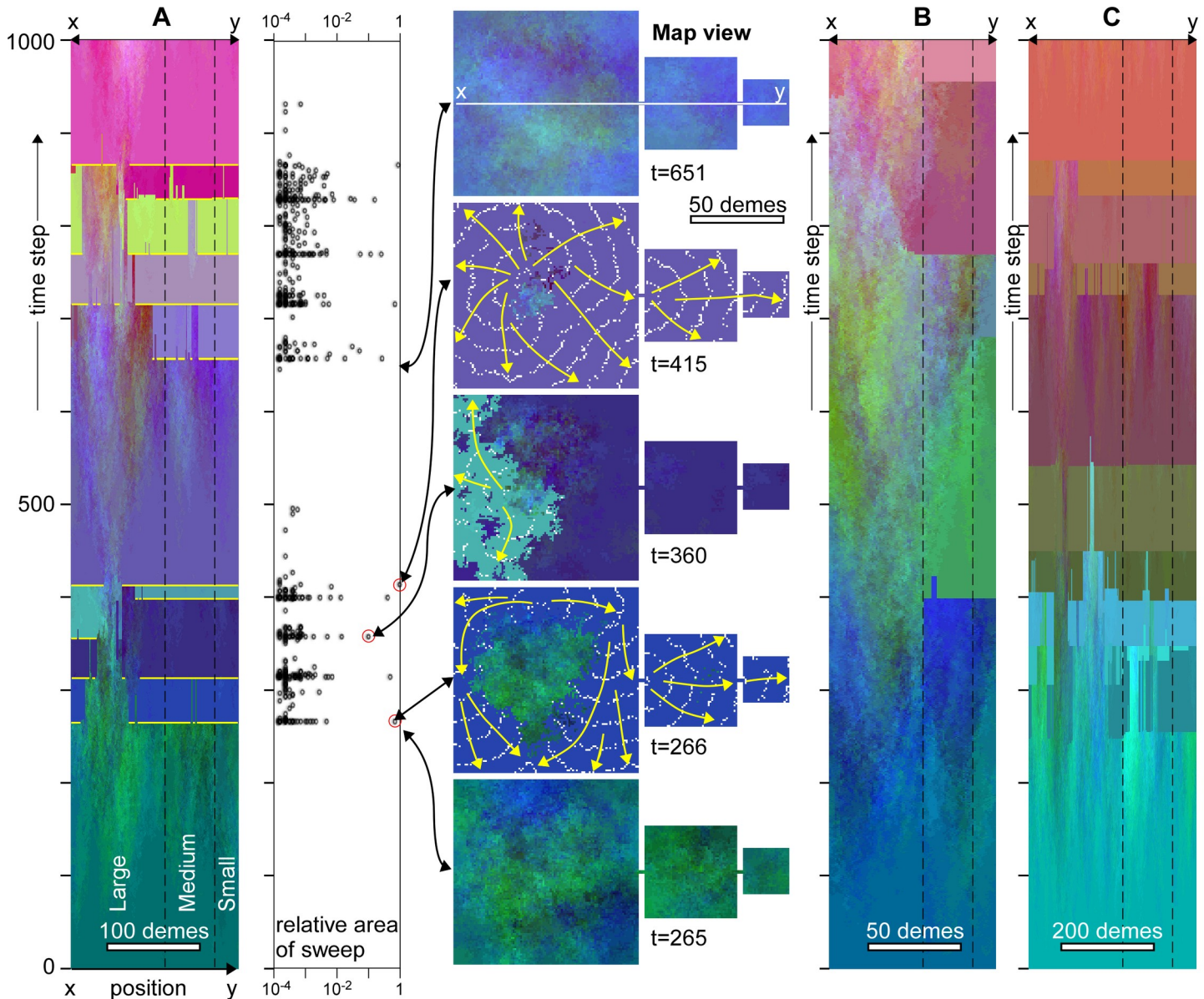

Fig 4. Evolution of genetic signatures in case of replacement sweeps as in Fig 3, but now with additional assortative mating. A. Temporal evolution along the line x-y through the centre of the model (see Fig 2). Sharp changes in colour indicate replacement sweeps. The main ones are highlighted in yellow. Note the overall continuity in time of genomes in the centre of the large continent that is rarely swept by migration waves. Graph shows the area (A_n, relative to total area) of individual sweeps as a function of time. Replacement sweeps are less clustered in time than in case of no assortative mating. Map views show the genetic distribution at five selected points in time. Direction and extent of three selected sweeps at t = 266, 360 and 415 are shown by yellow arrows and white lines that trace the front at regular intervals, respectively. These sweep events are highlighted with red circles in the A_n versus time graph. Doubling (**B**) or halving (**C**) the deme size roughly doubles or halves, respectively, the average time interval between clusters of replacement sweeps, but not the general pattern.

https://doi.org/10.1371/journal.pone.0201998.g004

a genetic continuity here. These demes have a higher fitness than the surrounding homogenised swept areas, and thus have a higher chance to initiate future sweeps. Marginal areas show distinct extinction events, as can be seen by distinct colour changes in Fig 4B. Halving or doubling the resolution has the expected effect of increasing, respectively decreasing the time between sweeps (Fig 4B and 4C).

Figs 3 and 4 show that marginal areas, in particular the small continent experience more sweeps than the centre of the area inside the large continent. The simulations shown in Figs 3A and 4A were also run for 10,000 steps, recording each time a deme was swept. Fig 5A shows that the chance for the two smaller continents and the margins of the large continent to be swept is about 1.5 times higher than in for the centre of the large continent in the absence of assortative mating. In case of assortative mating, the effect is even stronger. Demes in the centre of the largest continent thus have a much higher chance to be preserved, as these demes are rarely swept. This also affects the survival chance of mutations. The origins of mutations that reached fixation are plotted in Fig 5B. We see that these are strongly concentrated in the centre of the large continent. While this continent occupies 76% of the whole model area, it is the origin of >99% of all mutations that reached fixation. The medium continent with 19% of the area delivered only <1% of all mutations that reached fixation and the small continent not a single one. The chance of a mutation from the medium continent to reach fixation is only 3.5% that of a mutation in the large continent in the simulation without assortative mating. In the simulation with assortative mating this change reduced to 1.7%. Replacement sweeps thus strongly favour the survival of mutations from the centre of the largest populated landmass but not from the medium or small ones.

Directions of sweeps without (settings of Fig 3A) and with assortative mating (settings of Fig 4A) were recorded for simulations running 10,000 steps. Mean sweep propagation directions can be determined from this, and in turn, mean migration paths (Fig 5C). Migration paths consistently emanate from the centre of the large continent and lead to its margin and to
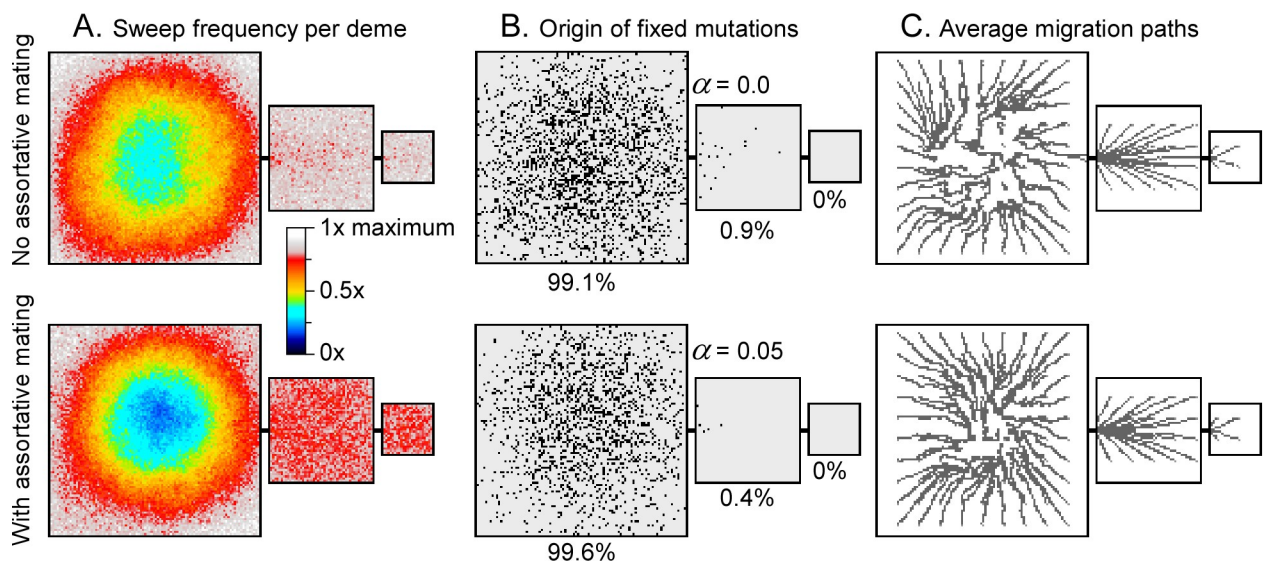

Fig 5. Origin of fixed mutations, as well as distribution and directions of sweeps. A. Relative frequency that a deme is swept by a migration wave. Demes on the margins and small continents are swept more often than demes in the centre of the large continent. These patterns are more pronounced in case of assortative mating (below) relative to the run without assortative mating. **B.** Origin of mutations that reached fixation shown at black dots on the map. Mutations that form in the middle of the large continent have a much larger chance of reaching fixation in the whole model area than mutations deriving from the margins, especially the small continent. **C.** Average directions of migrations within sweeps. Setting as in Figs 3A (top) and 4A (bottom), run for 10,000 steps. C.

https://doi.org/10.1371/journal.pone.0201998.g005

the smaller continents. Migration directions are more consistent in case of assortative mating, resulting in a more consistent pattern of paths in the centre of the large continent.

Fixation rate variation

After an initial period in which the system settles to a dynamic equilibrium, the number (N_{fix}) of mutations that reach fixation (i.e. spreading over entire model area) increases linearly with time (Fig 6). In the absence of replacement sweeps, N_{fix} increases steadily, whereas the N_{fix}-time curve is stairway-like with replacement sweeps. This is because large replacement sweeps spread some mutations over large areas, resulting in a sudden, but temporary increase in fixation events. As the fitness landscape is flattened after these events, few mutations can subsequently reach fixation until the process is repeated again.

The time-averaged fixation chance (P_{fix}) of an individual mutation is derived from the slope of the N_{fix}-time curve. P_{fix} is significantly lowered by replacement sweeps. With inter-breeding only, advantageous mutations are usually added to neighbouring genomes and few are lost by genetic drift before fixation, except at the nucleation phase just after the mutation occurred. Mutations in demes that are swept by replacement sweeps are lost, thus reducing the number of mutations that reach fixation [75]. Each wave causes a founder event, where only the limited genetic sample suddenly spreads over a large area [75–77]. The effect is more pronounced in case of assortative mating. The intersection of the linear regression of the N_{fix}-time curve with the horizontal time axis (Fig 6) gives the mean time to fixation (t_{fix}) for mutations that reach fixation. t_{fix} is about 4 times smaller in case of replacement sweeps than without these. This is to be expected, as replacement sweeps provide an efficient means to spread mutations over the map.

The reduced t_{fix} resulting from replacement sweeps has the advantage that a species can more quickly adapt to changes in the environment. This would cause some mutations to lose, and other to gain competitiveness. The latter can spread quickly in case of replacement sweeps. However, an inclination of a species towards replacements (low ΔF_{crit}) comes at a cost. Replacement sweeps imply that part of the population is excluded and inhibited from further
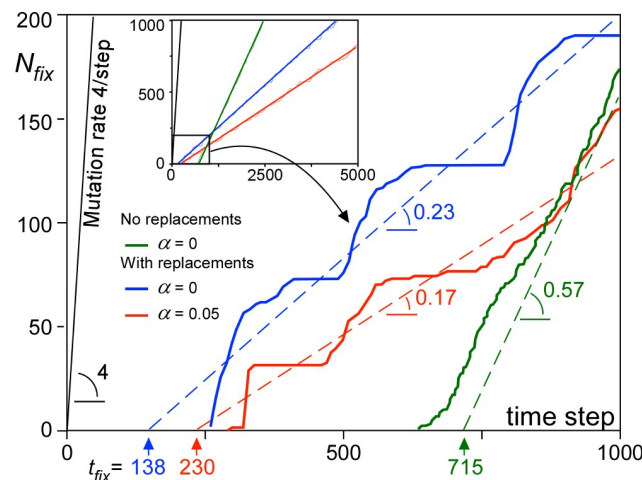

Fig 6. Number (N_{fix}) of mutations that reached fixation as a function of time with linear regression lines (for t>600 steps). Main graph shows the first 1000 time steps, while the inset shows graphs for the full 5000 time steps on which the linear regressions are based. Intersection of the linear regressions is the mean time to fixation (t_{fix}), while the slope is the rate at which mutations reach fixation. Replacement sweeps reduce the fixation chance of mutations by 60–70%, but also their t_{fix} by 3–5 times.

contributing to the species through their offspring. Furthermore, our simulations that are intentionally without any environmental changes show that a low ΔF_{crit} also leads to spontaneous replacement sweeps in the complete absence of any external factors.

Sweep area statistics

Although the largest sweeps are the most conspicuous in Figs 3 and 4, these are accompanied by many more smaller sweeps. Fig 7 shows the frequency (*f*) of sweep areas versus their normalised area (A_n = sweep area/model area). We see that that the data plot on a straight line in the double-log plot, indicating a power-law relationship between *f* and A_n, with an exponent -*q*:

$$f \propto (A_n)^{-q} \tag{8}$$

at least when A_n is small (up to a few per cent of the total area). A power law (Eq 8) was fitted to the data for $A_n < 0.01$ from simulations shown in Figs 3 and 4, but run for up to 10,000 steps, resulting in *q*-values ranging from 1.81 to 2.09. Frequencies were normalised such that the power-law best fit frequency for $A_n = 1$ is unity in each of the six simulations. All these normalised data together overlap remarkably well (Fig 7). We obtain *q* = 1.84 when applying a best fit to all data with $A_n < 0.01$. Normalised sweep areas >0.02 are overrepresented, with their frequencies up to >10x higher than the power-law trend. Notwithstanding this, small sweeps are several orders of magnitude more common than the largest ones.

The observed power-law relation is a hallmark of the self-organised criticality (SOC) model of Bak et al. [78] (but also see [79]) that has been used [74,80] to explain punctuated equilibria [73]. The classical SOC model is the (numerical) sand pile in which grains are randomly sprinkled on a stage. Once critical heights of grain piles, or gradients in these heights are reached, grains are redistributed locally. One redistribution event can lead to neighbouring sites reaching the criterion for redistribution, sometimes leading to large "avalanches". Sizes of these
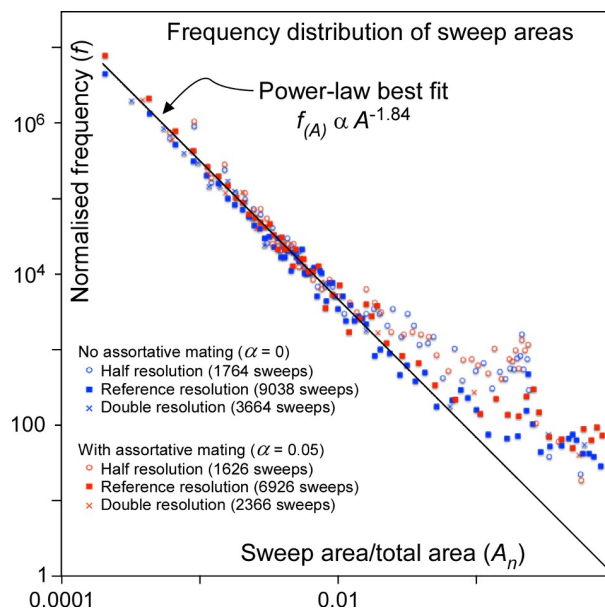

Fig 7. Normalised frequency distribution of areas swept by migration waves plotted against these areas (divided by total area) in a double-log plot. Data follow a power-law, except for the very largest sweeps. Dots represent the simulations with the schematic 3-continent map shown in Figs 3 and 4, but with 10,000 time steps.

avalanches typically follow power-law distributions [79,81], as the critical state has no intrinsic time or length scale [78]. The current model is similar to the classical sand-pile model, as mutations are "sprinkled" on the map of demes. There is a criterion for redistribution (ΔF_{crit}), which leads to replacement sweeps that indeed follow a power-law frequency distribution (Fig 8). A first difference with the standard sand-pile model is that, contrarily to grains, mutations can multiply. The second is that the model includes diffusion as an additional transport mechanism for mutations. Models with two transport channels, one fast avalanche-like and one diffusional, have been applied to fluid flow through pores and fractures [82–83], earthquake evolution [84–85], and heat transport in plasmas [86]. These models show that such systems still exhibit SOC-characteristics, as long as the criterion for the fast transport is frequently reached. However, with increasing importance of diffusion, avalanches become more regularly spaced in time and larger, isolated events (so-called "dragon kings" [87–88]) become more common [86]. This behaviour is indeed observed in our "mutation-pile" model, where large sweeps are over-represented compared to small ones and there is strong ($\alpha = 0$) and weak ($\alpha = 0.05$) cyclical behaviour with periods of semi-stasis (gradual diffusional differentiation), alternating with short periods of replacement sweeps. As such the model shows punctuated-equilibrium behaviour.

Although much scientific attention is devoted to large migration and extinction events, such as the expansion of AMH and the extinction of Neanderthals and Denisovans [26,32,45,69], smaller events have been recognised as well in Africa and Europe [28–31, 89–93]. The model predicts that if large sweeps can occur, a whole hierarchy of replacement sweeps of smaller ones should also occur. Unfortunately, the smaller these are, the more difficult these will be to discern in the fossil record. In view of the results presented here, the aforementioned evidence for such events in recent (Neolithic) times in Europe and Africa may be
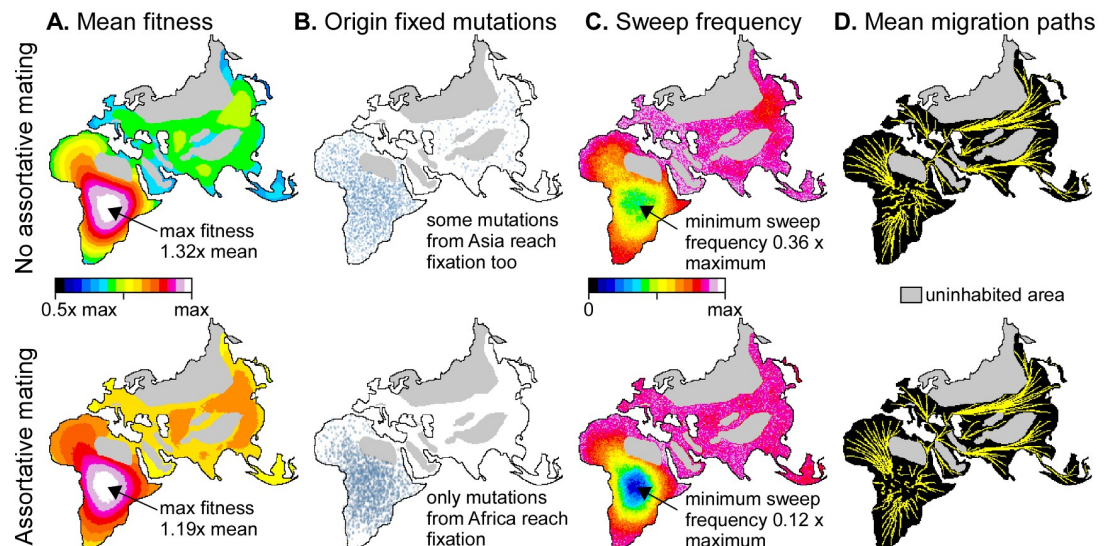

Fig 8. Example of applying the model for 10,000 steps with settings as in Figs 3A and 4A to a map of the Old World. Top row without ($\alpha = 0$) and bottom row with assortative mating ($\alpha = 0.05$). **A.** Mean fitness of demes over the whole simulation, showing that demes in Central Africa are, on average, fitter than the minimum at the margins of the populated area. **B.** Origin of all mutations that reached fixation. Most ($\alpha = 0$) or all ($\alpha = 0.05$) these mutations originated in Africa. **C.** Number of times that a deme has been swept by a migration wave. Demes in Central Africa experienced significantly fewer sweeps than the rest of the world, especially in case of $\alpha = 0.05$. **D.** Mean migration paths, all emanating from central Africa and diverging towards the periphery of the continent and into Asia.

regarded as supporting the hypothesis that small events were also common earlier in human evolution. Such small events should not be discarded as not important because of their local extent. Each time a sweep occurs and populations in the swept area become extinct, part of the genetic diversity is lost. This affects the accumulation rate of mutations and hence the molecular clock rate, which by it self is already difficult to determine [24,94–95]. Not recognising migration sweeps may lead to additional uncertainty in estimated molecular clock rates and resulting split times of phylogenetic split events, or in the estimate of the size of founder populations.

Parameter settings

The question of what the appropriate parameter settings (M, p, α, ΔF_{crit}) are can now be discussed as the effect of the various parameters was shown above. The advantage factor p determines the spreading rate of advantageous mutations by demic diffusion only. It depends on the competitive advantage (s) and population (N_D) of a deme, and, hence, on the assumed population density (ρ) and size of the demes (S). In combination with the mutation rate (M) it thus also determines the magnitude of gradients (ΔF) in the model. Actual values for M and s are largely unknown and in fact the "numerical mutations" would represent a number of real mutations with an effective competitive advantage of the ensemble. Depending on the choice of M and model resolution, p should be chosen such that the spreading rate is realistic. The scale of the three-continent model is comparable with that of the real world if we assume a deme size of $S = 50$ km. In that case the largest square continent would have an area of $25 \cdot 10^6$ km^2, comparable with Africa at ca. $30 \cdot 10^6$ km^2 and the middle one $6.25 \cdot 10^6$ km^2, somewhat smaller than Europe at ca. $10 \cdot 10^6$ km^2. The time step for a population density of between 0.1 and 1 individuals per km^2 results in a time step between $\Delta t \approx 400$ y and 4,000 y (Eq 2). The simulations in Figs 2 and 3 would then range between 400 ky and 4 My. Using $M = 4$, $p = 0.05$ results in spreading of mutations over significant distances (up to thousands of km) in periods of around a hundred thousands of years, but only when population density is low. Choosing a higher value for M would need to be compensated by a lower value of p to achieve the same spreading rate. The value of M also determines memory use and computation time, as does increasing the spatial resolution of the model (which reduces the time step; Eq 2). The choice of p thus depends on the assumed spreading rate of mutations by demic diffusion, in combination with the desired resolution in genomic signatures, time and space, bearing in mind computational capacities in terms of memory use and calculation time.

The choice of ΔF_{crit} depends on those of M, p and S, since these determine the magnitude of gradients and the time for these to develop. The number of migration sweeps is inversely proportional with ΔF_{crit}. Although the total number of sweeps is unknown (as many are too small to be resolved in the fossil or archaeological record), the number of very large ones (such as the spread of AMH) may be constrained to one or a few in the last few hundred thousands of years. This constraint enables setting the ΔF_{crit} to achieve the desired frequency of large events. The assortative mating factor (α) should also be set according to the various parameters that determine the magnitude of gradients. The choice of α depends on the expected efficacy of assortative mating and the size of homogeneous areas ("nations") that develop as a result. With the settings used here, $\alpha = 0.05$ results in homogenous areas that span in the order of hundreds to thousands of kilometres (Fig 2B), when not disturbed by replacement sweeps (Fig 4). In the current approach (Eq 1), assortative mating completely inhibits admixture between adjacent regions when $|\Delta G| \geq 1/2\alpha$. Genetic analyses, however, indicate admixture between hominin species, such as Neanderthals, Denisovans and AMH [24,96–97], but also admixture of more archaic into more modern AMH in Africa [29,98]. This could be included in the future by

replacing (Eq 1) with an exponential function for the decay of genetic exchange as a function of increasing |ΔG|, in which case the exchange probability never reaches zero. It should, however, be borne in mind that the purpose of this study is not to determine what the specific parameters are for human evolution, but to show what the effects of the different parameters are on the patterns of evolution.

Application to a world map

Having assessed the effects of, and patterns resulting from the different parameters on a schematic map with three continents, we now briefly apply the model to a real-world map. For this purpose we used a Fuller-projection map of the Old World (Fig 8), roughly adapted to ice age conditions by linking Japan and the British Isles to the mainland and assuming that large parts of northern Europe and Asia are (effectively) not inhabited. Although population densities (ρ) would never have been equal throughout the inhabited area, we maintain the assumption of a constant ρ, but excluded high-elevation areas (especially Tibet and the Pamirs) and desert areas in North Africa and the Arabian Peninsula, adapted from Eriksson et al. [39] for ~21 ka BP. In this configuration inhabited areas in Africa occupy 44% of the whole inhabited area. Inhabited areas evidently varied over time, but this simplified model serves the purpose of predicting the main expected patterns. Deme size was set at 50x50 km, resulting in 20808 populated demes, and settings were equal to those for the simulations shown in Figs 3A and 4A. At a time step of about 4000 years (for $\rho = 0.01$ individuals/km^2), $p = 0.05$ would lead to a mutation spreading rate of 0.002 km/yr (Eq 5). Replacement sweeps in the current model take place within one time step. The maximum distance to travel, from South Africa to Japan is about 17,500 km, resulting in a maximum sweep velocity of ~4 km/yr. Such high velocities, however, only apply to the few very largest sweeps. To achieve good statistics, the models are run for 10,000 time steps, thus representing ca. 40 million years, which is in the order of about 40 real-world evolutions.

In both simulations, with and without assortative mating, mean fitness is highest in central Africa (Fig 8A). The fitness maximum is most distinct in case of $\alpha = 0$, because the long and regular interval between clusters of sweep events allow large-scale gradients to develop. Mutations that reach fixation mostly come from central Africa (Fig 8B). When $\alpha = 0.05$ no mutations that originated outside of Africa reach fixation. When $\alpha = 0$, a few mutations from Asia reach fixation, because sweeps from Africa can trigger "counter" sweeps after admixture with genomes from the margin of the swept areas. The chance that a deme in central Africa is swept by a migration event is higher in case of $\alpha = 0$ than when $\alpha = 0.05$ (Fig 8C). Despite these differences, migration directions are mostly emanating from central Africa in the direction of the margins of the occupied area (Fig 8D).

Sweep area frequencies follow the same power-law distribution (Eq 8 and Fig 9A) as in the abstract 3-continent model. Largest sweeps are again over-represented relative to the power-law trend for smaller sweeps. The effect becomes noticeable for sweeps that are larger than a few per cent of the total area. This is about 1/3 the area of Europe. The frequency distributions show two distinct peaks. One is at the area of Japan, which in the model forms a narrow peninsula connected to Asia. Sweeps apparently initiate at the connection with the peninsula (where mutations rarely occur) and then tend to sweep the whole peninsula. The second peak is at about 56% of the total area, which equals the area of Eurasia. This indicates that isthmuses, such as the Sinai Peninsula, play an important bottleneck role and sweeps from Africa that entered Asia have an increased chance of then sweeping the whole of Eurasia.

The cumulative number of sweeps as a function of area (Fig 9B) shows that sweeps of the size of Eurasia or larger represent about 1% of all sweeps. However, these few sweeps are
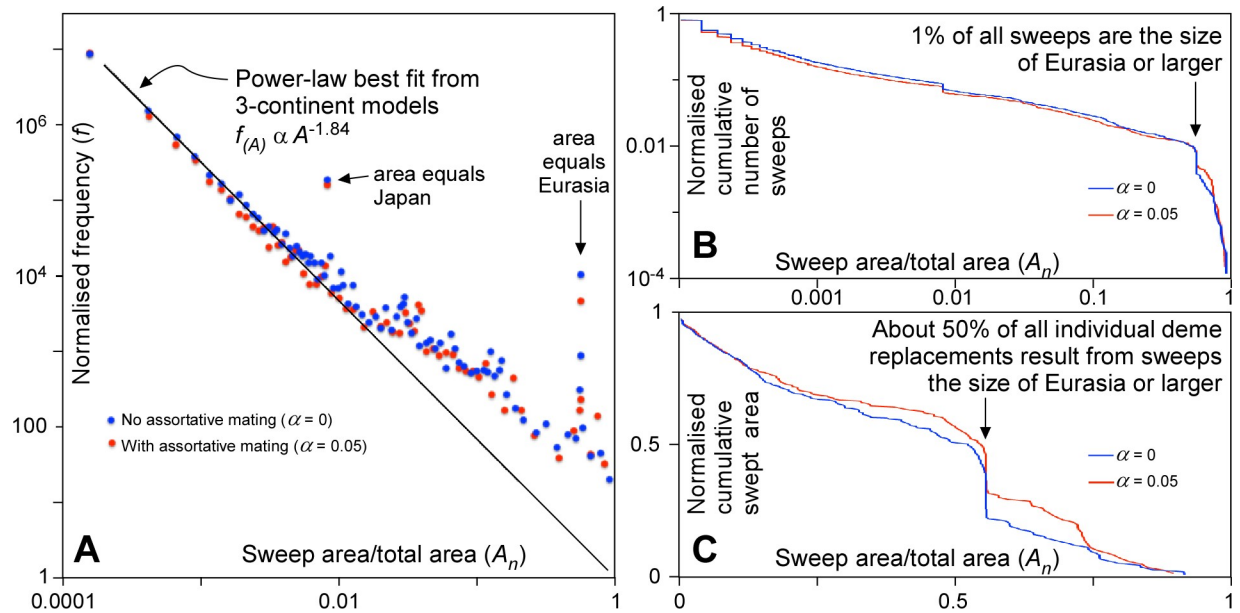
Fig 9. Sweep statistics of simulations for the old world. A. Graph of normalised frequency as a function of sweep area. **B.** Cumulative graph of number of sweeps against sweep area. About 1% of all sweeps are the size of Eurasia (56% of total area) or larger. **C.** Cumulative graph of the areas swept as a function of sweep area. About 50% of all individual deme replacements result from sweeps are the size of Eurasia (56% of total area) or larger.

https://doi.org/10.1371/journal.pone.0201998.g009

responsible for about 50% of all individual deme replacement events over time (Fig 9C). If in the past there were one or two major out-of-Africa sweeps, one can deduce that there were in the order of 100–200 replacement sweeps in total. The average number of sweeps that an individual population in one single deme would have experienced would be about 2–4, double the number of very large sweeps. Two to four replacement events in a million years, i.e. ~40,000 generations, means that individuals in a deme have a chance in the order of 0.005–0.01% of experiencing a replacement sweep in their lifetime. Although sweeps thus rarely affect individuals, they have a profound effect on the evolution of the human genome, because about half these locally experienced sweeps are part global-scale sweeps that span a significant part of the whole populated Old World.

Future extensions of the model

The model employed here intentionally excluded environmental or other external factors, with the exception of geographical barriers, such as coastlines, deserts and high mountains. This does not imply that the model is restricted to this simplification. Incorporation of environmental factors requires population densities that can vary in space and time. It is envisaged to include a carrying capacity, which is a function of environment, but potentially also of the genetic signature. For this purpose, mutations could be assigned variable "fitness", depending on the environment. These factors can be used to determine population density changes. Eqs (1) and (2) are currently based on the assumption that two neighbouring demes have the same population. These equations can be adapted to relax this assumption. The framework of the model is furthermore amenable to multiple competing populations or species that occupy a single deme. These extensions of the model are not restricted to human evolution. However, the model is particularly suitable for studying the emergence of modern humans, because mutations in the numerical genome may also represent cultural traits or innovations. These

can be assigned their own mutation and diffusion rates, advantageousness (possibly related to environment), as well as effect on assortative mating and initiation of replacement waves. This will allow exploring the interaction between biological and cultural evolution [99–102].

Conclusions

Diffusional gene flow alone leads to a homogenisation of all populations [103]. However, ongoing mutations continuously produce local variations that take time to spread over the whole populated area. The combination of diffusion and mutations thus results in isolation by distance [71], with differences between local populations increasing with distance (Fig 2A). The magnitude of these differences or clines depends on the balance between diffusion and mutation rate. The effect of assortative mating is to create a structured population [70] with relatively homogeneous "nation" regions, separated by distinct clines. While Scerri et al. [70] argue that the structuring is due to environmental and ecological drivers, our model (Fig 2B) shows that population structuring could be developed due to the neutral process of assortative mating without any such additional drivers. Without other evolutionary mechanisms, assortative mating reduces or inhibits exchange between regions and this exchange is restricted to neighbouring regions. Migration events are an efficient way to bring populations from far-removed regions into contact. Ensuing exchange across such new contacts leads to reticulate phylogenies [67].

Our model shows that, if population/species replacements do occur, replacement sweeps of all sizes up to the whole populated area are expected. The basic reason is that if one group of individuals can take over the area of their neighbours, the chance that they (or their offspring) can also take over the next area is larger than zero. This can, but must not, lead to "avalanches" of replacements that can span up to the whole populated area. Replacement-sweep-area frequencies systematically decrease as a power-law function of their area. For every world-spanning sweep, about two orders of magnitude smaller sweeps are to be expected, down to the size of one deme in the model. As expected, isthmuses appear to play a special "bottle neck" role during expansions. Once a sweep crosses an isthmus, there is an increased chance that the whole peninsula beyond is swept in its entirety. In simulations this leads to a distinct peak in the chance that the whole of Eurasia is swept in at an out-of-Africa event.

Replacement sweeps reduce the chance of fixation of mutations, but also significantly reduce the time to fixation of those mutations that do finally reach fixation. The propensity of a population to usurp the area of its neighbours if these are, for some reason, less competitive, has the benefit that advantageous mutations can quickly spread, for example after a change in environmental conditions. However, our simulations show that this propensity inevitably also leads to spontaneous replacement sweeps that are not triggered by any external factors but driven by genetic drift.

Our simulations show that replacement sweeps mostly emanate from the largest consolidated populated area. In the Old World this is Africa, especially during glaciation stages. The simulations indicate that the most likely origin for modern humans lies somewhere in (central) Africa, in line with what is deduced from the fossil record (e.g. [104]). However, East Asia also forms large and compact populated area, especially during warm periods, that would have been a second probable source for replacement sweeps. This emphasizes the need for further palaeoanthropological research in East Asia (e.g. [5,105]).

Large migration sweeps generally emanate from the central regions of large compact areas and spread towards the margins. The spreading directions are mostly determined by coastlines, mountains and other uninhabited areas. This leads to a remarkable consistency of the directions, quite independent of the parameter settings (Fig 8C). The tendency to migrate

towards coasts is consistent with the beachcomber model [106]. The spreading of a migration wave is more like that of an inkblot than along narrow, bifurcating migration paths that some authors envisage [107].

Mutations that arise in the centre of large compact areas have the highest change to survive and spread. This is not only because these areas are the probably sources of migration sweeps, but they are also the least likely to be swept themselves (Fig 8C). This pattern illustrates the relevance of the central areas as potential sources of new variants, but also in preserving old traits.

Considering a combination of semi-stasis periods alternating with replacement sweeps as a result of large-scale and many smaller expansions may contribute to understand the current biological distribution of human populations, as well as the variation in the hominin fossil record. For this reason we suggest an integration of concepts coming from punctuated equilibrium theory [72,74,79–80], multiregional postulates [25,66– 67,70,93], and current out-of-Africa migration models. Any migration wave that spanned the whole world is most likely to have come from Africa. If large migration waves can occur, more numerous smaller waves are to be expected too. Multiple out-of-Africa waves are, therefore, most likely if one happened. Although the propensity for replacement waves makes a species more adaptable to changes in its environment, a "side effect" is that such waves then also occur spontaneously. A spontaneous emergence and spread of modern humans from Africa should thus be regarded as a null hypothesis against which any hypothetical causes should be tested.

Supporting information

S1 Fig. Determination of the relationship between *p* and *s*, as well as the model time step. A. The factor *p* as a function of competitive advantage *s* and population size *N*. Each data point is represents the average 10,000 simulations for a give *N* and *s*. Slopes (*dP/ds*) are determined by linear least-squares best fits (dashed lines). **B.** A regression (dashed line) shows that *dP/ds* is a linear function of *N*. **C.** Modelled mean time to fixation of a neutral mutation is found to be a linear function of *N*.
(TIF)

S2 Fig. Workflow of the numerical implementation of the model. Individual loops are given in different colours.
(TIF)

S1 File. Supporting information on methods. The text explains the relationship between advantage factor (*p*) and competitive advantage (*s*) and how the duration of one time step (Δ*t*) is derived.
(PDF)

Acknowledgments

Author Contributions

Conceptualization: Paul D. Bons, Catherine C. Bauer, Hervé Bocherens, Tamara de Riese, Dorothée G. Drucker, Michael Francken, Lumila Menéndez, Alexandra Uhl, Christoph Wißing.

Formal analysis: Paul D. Bons, Boudewijn P. van Milligen.

Investigation: Paul D. Bons, Catherine C. Bauer, Lumila Menéndez.

Methodology: Paul D. Bons, Tamara de Riese, Boudewijn P. van Milligen.

Project administration: Paul D. Bons.

Software: Paul D. Bons, Tamara de Riese.

Validation: Paul D. Bons.

Visualization: Paul D. Bons.

Writing – original draft: Paul D. Bons.

Writing – review & editing: Paul D. Bons, Catherine C. Bauer, Hervé Bocherens, Tamara de Riese, Dorothée G. Drucker, Lumila Menéndez, Alexandra Uhl, Christoph Wißing.

References

1. Tattersall I. Paleoanthropology: the last half-century. Evol Anthropol. 2000; 9: 2–16.

2. Foley R. In the shadow of the modern synthesis? Alternative perspectives on the last fifty years of paleoanthropology. Evol Anthropol. 2001; 10: 5–14.

3. Bräuer G. The origin of modern anatomy: by speciation or intraspecific evolution? Evol Anthropol. 2008; 17: 22–37.

4. Dennell RW. The colonization of "Savannahstan": issues of timing(s) and patterns of dispersal across Asia in the Late Pliocene and Early Pleistocene. In: Asian Paleoanthropology. Springer, Dordrecht; 2011. 7–30.

5. Zhu Z, Dennell R, Huang W, Wu Y, Qiu S, Yang S, et al. Hominin occupation of the Chinese Loess Plateau since about 2.1 million years ago. Nature. 2018; https://doi.org/10.1038/s41586-018-0299-4 PMID: 29995848

6. White TD, Asfaw B, DeGusta D, Gilbert H, Richards GD, Suwa G, et al. Pleistocene Homo sapiens from Middle Awash, Ethiopia. Nature. 2003; 423: 742–747. https://doi.org/10.1038/nature01669 PMID: 12802332

7. McDougall I, Brown FH, Fleagle JG. Stratigraphic placement and age of modern humans from Kibish, Ethiopia. Nature. 2005; 433: 733–736. https://doi.org/10.1038/nature03258 PMID: 15716951

8. Hublin JJ, Ben-Ncer A, Bailey SE, Freidline SE, Neubauer S, Skinner MM, et al. New fossils from Jebel Irhoud, Morocco and the pan-African origin of *Homo sapiens*. Nature. 2017; 546: 289–292. https://doi.org/10.1038/nature22336 PMID: 28593953

9. Lahr MM, Foley R. Multiple dispersals and modern human origins. Evol Anthropol. 1994; 3: 48–60.

10. Conard NJ, Bolus M. Radiocarbon dating the appearance of modern humans and timing of cultural innovations in Europe: new results and new challenges. J Hum Evol. 2003; 44: 331–371. PMID: 12657520

11. Hershkovitz I, Weber GW, Quam R, Duval M, Grün R, Kinsley L, et al. The earliest modern humans outside Africa. Science. 2018; 359: 456–459. https://doi.org/10.1126/science.aap8369 PMID: 29371468

12. Mellars P, French, CJ. Tenfold Population Increase in Western Europe at the Neandertal–to–Modern Human Transition. Science. 2011; 333: 623–627. https://doi.org/10.1126/science.1206930 PMID: 21798948

13. Groucutt HS, Petraglia MD, Bailey G, Scerri EM, Parton A, Clark-Balzan L, et al. Rethinking the dispersal of Homo sapiens out of Africa. Evol Anthropol: Issues, News, and Reviews. 2015; 24(4): 149–164.

14. Prat S. First hominin settlements out of Africa. Tempo and dispersal mode: Review and perspectives. Comptes Rendus Palevol. 2018; 17: 6–16.

15. Krings M, Stone A, Schmitz RW, Krainitzki H, Stoneking M, Pääbo S. Neanderthal DNA sequences and the origin of modern humans. Cell. 1997; 90(1): 19–30. PMID: 9230299

16. Krings M, Geisert H, Schmitz RW, Krainitzki H, Pääbo S. DNA sequence of the mitochondrial hypervariable region II from the Neanderthal type specimen. Proc Natl Acad Sci U S A. 1999; 96: 5581–5585. PMID: 10318927

17. Krings M, Capelli C, Tschentscher F, Geisert H, Meyer S, Haeseler A. A view of Neanderthal genetic diversity. Nat Genet. 2000; 26: 144–146. https://doi.org/10.1038/79855 PMID: 11017066

18. Brown P, Sutikna T, Morwood MJ, Soejono RP, Jatmiko E, Wayhu Saptomo E., et al. A new small-bodied hominin from the Late Pleistocene of Flores, Indonesia. Nature. 2004; 431: 1055–1061. https://doi.org/10.1038/nature02999 PMID: 15514638

19. Morwood MJ, Soejono RP, Roberts RG, Sutikna T, Turney CSM, Westaway KE, et al. Archaeology and age of a new hominin from Flores in eastern Indonesia. Nature. 2004; 431: 1087–1091. https://doi.org/10.1038/nature02956 PMID: 15510146

20. Morwood MJ, Brown P, Sutikna T, Saptomo EW, Westaway KE, Due RA, et al. Further evidence for small-bodied hominins from the Late Pleistocene of Flores, Indonesia. Nature. 2005; 437: 1012–1017. https://doi.org/10.1038/nature04022 PMID: 16229067

21. Krause J, Orlando L, Serre D, Viola B, Prüfer K, Richards MP, et al. Neanderthals in central Asia and Siberia. Nature. 2007; 449: 902–904. https://doi.org/10.1038/nature06193 PMID: 17914357

22. Krause J, Fu Q, Good JM, Viola B, Shunkov MV, Derevianko AP, et al. The complete mitochondrial DNA genome of an unkown hominin from southern Siberia. Nature. 2010; 464: 894–897. https://doi.org/10.1038/nature08976 PMID: 20336068

23. Higham T, Douka K, Wood R, Ramsey CB, Brock F, Basell L, et al. The timing and spatiotemporal patterning of Neanderthal disappearance. Nature. 2014; 512: 306–309. https://doi.org/10.1038/nature13621 PMID: 25143113

24. Posth C, Wißing C, Kitagawa K, Pagani L, van Holstein L, Racimo F, et al. Deeply divergent archaic mitochondrial genome provides lower time boundary for African gene flow into Neanderthals. Nat Commun. 2017; 8: 16046. https://doi.org/10.1038/ncomms16046 PMID: 28675384

25. Cavalli-Sforza LL, Menozi P, Piazza A. Demic expansions and human evolution. Science. 1993; 259: 639–646. PMID: 8430313

26. Hublin JJ. The modern human colonization of western Eurasia: when and where? Quat Sci Rev. 2015; 118: 194–210.

27. Nigst PR, Haesaerts P, Damblon F, Frank-Fellner C, Mallol C, Viola B, et al. Early modern human settlement of Europe north of the Alps occurred 43,500 years ago in a cold steppe-type environment. PloS ONE. 2014; 111: 14394–14399.

28. Reed FA, Tishkoff SA. African human diversity, origins and migrations. Curr Opin Genet Dev. 2006; 16: 597–605. https://doi.org/10.1016/j.gde.2006.10.008 PMID: 17056248

29. Skoglund P, Thompson JC, Prendergast ME. Reconstructing Prehistoric African Population Structure. Cell. 2017; 171: 59–71. https://doi.org/10.1016/j.cell.2017.08.049 PMID: 28938123

30. Fu Q, Posth C, Hajdinjak M, Petr M, Mallick S, Fernandes D, et al. The genetic history of Ice Age Europe. Nature. 2016; 534: 200–205. https://doi.org/10.1038/nature17993 PMID: 27135931

31. Posth C, Renaud G, Mittnik A, Drucker DG, Rougier H, Cupillard C, et al. Pleistocene Mitochondrial Genomes Suggest a Single Major Dispersal of Non-Africans and a Late Glacial Population Turnover in Europe. Curr Biol. 2016; 26: 827–833. https://doi.org/10.1016/j.cub.2016.01.037 PMID: 26853362

32. Banks WE, d'Errico F, Peterson AT, Kageyama M, Sima A, Sanchez-Goni MF. Neanderthal extinction by competitive exclusion. PloS ONE. 2008; 3(12): e3972. https://doi.org/10.1371/journal.pone.0003972 PMID: 19107186

33. Agustí J, Rubio-Campillo X. Were Neanderthals responsible for their own extinction? Quat Int. 2017; 431: 232–237.

34. Gilpin W, Feldman MW, Aoki K. An ecocultural model predicts Neanderthal extinction through competition with modern humans. Proc Natl Acad Sci U S A. 2016; 113(8): 2134–2139. https://doi.org/10.1073/pnas.1524861113 PMID: 26831111

35. d'Errico F, Sánchez Goñi MF. Neandertal extinction and the millennial scale climatic variability of OIS 3. Quat Sci Rev. 2003; 22: 769–788.

36. Tzedakis PC, Hughen KA, Cacho I, Harvati K. Placing late Neanderthals in a climatic context. Nature. 2007; 449: 206–208. https://doi.org/10.1038/nature06117 PMID: 17851522

37. Müller UC, Pross J, Tzedakis PC, Gamble C, Kotthoff U, Schmiedl G, et al. The role of climate in the spread of modern humans into Europe. Quat Sci Rev. 2011; 30: 273–279.

38. Rosenberg TM, Preusser F, Fleitmann D, Schwalb A, Penkman K, Schmid TW, Al-Shanti MA, Kadi K, Matter A. Humid periods in southern Arabia: Windows of opportunity for modern human dispersal. Geology. 2011; 39: 1115–1118.

39. Eriksson A, Betti L, Friend AD, Lycett SJ, Singarayer JS, von Cramon-Taubadel N, Valdes PJ, Balloux F, Manica A. Late Pleistocene climate change and the global expansion of anatomically modern

humans. Proc Natl Acad Sci U S A. 2012; 109: 16089–16094. https://doi.org/10.1073/pnas.1209494109 PMID: 22988099

40. Grove M, Lamb H, Roberts H, Davies S, Marshall M, Bates R, et al. Climatic variability, plasticity, and dispersal: A case study from Lake Tana, Ethiopia. J Hum Evol. 2015; 87: 32–47. https://doi.org/10.1016/j.jhevol.2015.07.007 PMID: 26472274

41. Maslin MA, Shultz S, Trauth MH. A synthesis of the theories and concepts of early human evolution. Phil Trans R Soc B. 2015; 370: 20140064. http://dx.doi.org/10.1098/rstb.2014.0064 PMID: 25602068

42. Timmermann A, Friedrich T. Late Pleistocene climate drivers of early human migration. Nature. 2016; 538, 92–95. https://doi.org/10.1038/nature19365 PMID: 27654920

43. Lamb HF, Bates CR, Bryant CL, Davies SJ, Huws DG, Marshall MH, et al. 150,000-year palaeoclimate record from northern Ethiopia supports early, multiple dispersals of modern humans from Africa. Sci Rep. 2018; 8(1): 1077. https://doi.org/10.1038/s41598-018-19601-w PMID: 29348464

44. Agustí J, Blain H-A, Cuenca-Bescós G. Bailon S. Climate forcing of first hominid dispersal in Western Europe. J Hum Evol. 2009; 57: 815–821. https://doi.org/10.1016/j.jhevol.2009.06.005 PMID: 19683790

45. Kolodny O, Feldman MW. A parsimonious neutral model suggests Neanderthal replacement was determined by migration and random species drift. Nat Commun. 2017; 8(1): 1040. https://doi.org/10.1038/s41467-017-01043-z PMID: 29089499

46. Bocquet-Appel JP, Demars PY. Population Kinetics in the Upper Palaeolithic in Western Europe. J Archaeol Sci. 2000; 27: 551–570, https://doi.org/10.1006/jasc.1999.0471

47. Bocquet-Appel JP, Demars PY, Noiret L. Dobrowsky D. Estimates of Upper Palaeolithic meta-population size in Europe from archaeological data. Journal of Archaeological Science. 2005; 32: 1656–1668, https://doi.org/10.1016/j.jas.2005.05.006

48. Bocquet-Appel JP, Degioanni A. Neanderthal Demographic Estimates. Curr Anthropol. 2013; 54: S202–S213, https://doi.org/10.1086/673725

49. Blum MGB, Jakobsson M. Deep Divergences of Human Gene Trees and Models of Human Origins. Mol Biol Evol. 2011; 28; 889–898, https://doi.org/10.1093/molbev/msq265 PMID: 20930054

50. Hoban S, Bertorelle G, Gaggiotti OE. Computer simulations: tools for population and evolutionary genetics. Nat Rev. 2012; 13: 110–122. https://doi.org/10.1038/nrg3130 PMID: 22230817

51. Lake MW. Trends in archaeological simulation. J Arch Method Theory. 2014; 21: 258–287.

52. Liu H, Prugnolle F, Manica A, Balloux F. A geographically explicit genetic model of worldwide human-settlement history. Am J Hum Genet. 2006; 79: 230–237. https://doi.org/10.1086/505436 PMID: 16826514

53. Ray N, Currat M, Foll M, Excoffier L. SPLATCHE2: A spatially explicit simulation framework for complex demography, genetic admixture and recombination. Bioinformatics. 2010; 26: 2993–2994. https://doi.org/10.1093/bioinformatics/btq579 PMID: 20956243

54. Barton CM, Riel-Salvatore J. Agents of change: modeling biocultural evolution in Upper Pleistocene western Eurasia. Adv Complex Syst. 2012; 15: 1150003, https://doi.org/10.1142/S0219525911003359

55. Benguigui M, Arenas M. Spatial and Temporal Simulation of Human Evolution. Methods, Frameworks and Applications. Curr Genomics. 2014; 15: 245–255. https://doi.org/10.2174/1389202915666140506223639 PMID: 25132795

56. Rikvold PA, Zia RKP. Punctuated equilibria and 1/f noise in a biological coevolution model with individual-based dynamics. Phys Rev E. 2003; 68: 031913, https://doi.org/10.1103/PhysRevE.68.031913 PMID: 14524809

57. Filotas E, Grant M, Parrott L, Rikvold PA. Positive interactions and the emergence of community structure in metacommunities. J Theoret Biol. 2010; 266: 419–429.

58. Whitlock MC. Fixation Probability and Time in Subdivided Populations. Genetics. 2003; 164: 767–779. PMID: 12807795

59. Fisher RA. The Genetical Theory of Natural Selection. Oxford: Oxford University Press; 1930.

60. Fisher RA. The wave of advance of advantageous genes. Ann Eugen. 1937; 7: 355–369. https://doi.org/10.1111/j.1469-1809.1937.tb02153.x

61. Kimura O, Ohta T. The average number of generations until fixation of a mutant gene in a finite population. Genetics. 1969; 61: 763–771. PMID: 17248440

62. Gavrilets S. Perspective: Models of speciation: what have we learned in 40 years? Evolution. 2013; 57: 2197–2215.

63. Haldane JBS. A mathematical theory of natural and artificial selection. V Proc Camb Philos Soc. 1927; 23:838–844.

64. Wright S. Evolution in Mendelian populations. Genetics. 1931; 16: 97–159. PMID: 17246615

65. Lande R. Natural selection and random genetic drift in phenotypic evolution. Evolution. 1976; 30: 314–334. https://doi.org/10.1111/j.1558-5646.1976.tb00911.x PMID: 28563044

66. Wolpoff MH, Hawks J, Caspari R. Multiregional, Not Multiple Origins. Am J Phys Anthropol. 2000; 112: 129–136 https://doi.org/10.1002/(SICI)1096-8644(200005)112:1<129::AID-AJPA11>3.0.CO;2-K PMID: 10766948

67. Winder IC, Winder NP. Reticulate evolution and the human past: an anthropological perspective. Ann Hum Biol. 2014; 41: 300–311, https://doi.org/10.3109/03014460.2014.922613 PMID: 24932745

68. Bae CJ, Douka K, Petraglia MD. Human Colonization of Asia in the Late Pleistocene–An introduction to Supplement 17. Curr Anthropol. 2017; 58(17): S373 –S382.

69. Galway-Witham J, Stringer C. How did Homo sapiens evolve? Science. 2018; 360: 1296–1298 https://doi.org/10.1126/science.aat6659 PMID: 29930123

70. Scerri EML, Thomas MG, Manica A, Gunz P, Stock JT, Stringer C. Did Our Species Evolve in Subdi-vided Populations across Africa, and Why Does It Matter? Trends Ecol Evol. 2018; https://doi.org/10.1016/j.tree.2018.05.005 PMID: 30007846

71. Shennan SJ, Crema ER, Kerig T. Isolation-by-distance, homophily and 'core' vs. 'package' cultural evolution models in Neolithic Europe. Evol Hum Behav. 2015; 36: 103–109

72. Gould SJ, Eldredge N. Punctuated equilibria: the tempo and mode of evolution reconsidered. Paleobi-ology. 1977; 3: 115–151;

73. Gould SJ, Eldredge N. Punctuated equilibrium comes of age. Nature. 1993; 366: 223–227 https://doi.org/10.1038/366223a0 PMID: 8232582

74. Bak P, Boettcher S. Self-organized criticality and punctuated equilibria. Physica D. 1997; 107: 143–150.

75. Excoffier L, Foll M, Petit RJ. Genetic Consequences of Range Expansions. Annu Rev Ecol Evol Syst. 2009; 40: 481–501.

76. Ramachandran S, Deshpande O, Roseman CC, Rosenberg NA, Feldman MW, Cavalli-Sforza LL. Support from the relationship of genetic and geographic distance in human populations for a serial founder effect originating in Africa. Proc Natl Acad Sci. 2005; 102:15942–15947. https://doi.org/10.1073/pnas.0507611102 PMID: 16243969

77. Sugden LA, Ramachandran S. Integrating the signatures of demic expansion and archaic introgres-sion in studies of human population genomics. Curr Opin Genet Dev. 2016; 41:140–149 https://doi.org/10.1016/j.gde.2016.09.007 PMID: 27743539

78. Bak P, Tang C, Wiesenfeld K. Self-organized criticality, Phys Rev A. 1988; 38: 364–374.

79. Murase Y, Rikvold PA, Conservation of population size is required for self-organized criticality in evolu-tion models. New J Phys. 2018; 20: 083023. https://doi.org/10.1088/1367-2630/aad861

80. Bak P, Sneppen K. Punctuated Equilibrium and Criticality in a Simple Model of Evolution. Phys Rev Lett. 1993; 71: 4083–4086. https://doi.org/10.1103/PhysRevLett.71.4083 PMID: 10055149

81. Solé RV, Manrubia SC, Benton M, Bak P. Self-similarity of extinction statistics in the fossil record. Nature. 1997; 388: 764–767.

82. Miller SA, Nur A. Permeability as a toggle switch in fluid-controlled crustal processes. Earth Planet Sci Lett. 2000; 183(1–2): 133–146.

83. Bons PD, van Milligen BP. A new experiment to model self-organized critical transport and accumula-tion of melt and hydrocarbons from their source rocks. Geology. 2001; 29: 919–922, https://doi.org/10.1130/0091-7613

84. Sornette A, Sornette D. Self-organized criticality and earthquakes. Europhys Lett. 1989; 9(3): 197.

85. Olami Z, Feder HJS, Christensen K. Self-organized criticality in a continuous, nonconservative cellular automaton modeling earthquakes. Phys Rev Lett. 1992; 68(8): 1244. https://doi.org/10.1103/PhysRevLett.68.1244 PMID: 10046116

86. Sánchez R, Newman DE, Carreras BA. Mixed SOC diffusive dynamics as a paradigm for transport in fusion devices. Nuclear Fusion. 2001; 41: 247–256.

87. Sachs MK, Yoder MR, Turcotte DL, Rundle JB, Malamud BD. Black swans, power laws, and dragon-kings: Earthquakes, volcanic eruptions, landslides, wildfires, floods, and SOC models. Eur Phys J Spec Top. 2012; 205: 167–182.

88. Sornette D, Ouillon G. Dragon-kings: mechanisms, statistical methods and empirical evidence. Eur Phys J Spec Top. 2012; 205(1): 1–26.

89. Campbell MC, Tishkoff SA. The evolution of human genetic and phenotypic variation in Africa. Curr Biol. 2010; 20: R166–R173. https://doi.org/10.1016/j.cub.2009.11.050 PMID: 20178763

90. Fu Q, Rudan P, Pääbo S, Krause J. Complete Mitochondrial Genomes Reveal Neolithic Expansion into Europe. PloS ONE. 2012; 7: 32473. https://doi.org/10.1371/journal.pone.0032473 PMID: 22427842

91. Hervella M, Rotea M, Izagirre N, Constantinescu M, Alonso S, Ioana M, et al. Ancient DNA from South-East Europe Reveals Different Events during Early and Middle Neolithic Influencing the European Genetic Heritage. PLoS ONE. 2015; 10: 0128810. https://doi.org/10.1371/journal.pone.0128810

92. Lazaridis I. The evolutionary history of human populations in Europe. Curr Opinion Genetics Develop. 2018; 53: 21–27.

93. Schlebusch CM, Malmström H, Günther T, Sjödin P, Coutinho A, Edlund H, et al. Southern African ancient genomes estimate modern human divergence to 350,000 to 260,000 years ago. Science. 2017; 358: 652–655. https://doi.org/10.1126/science.aao6266 PMID: 28971970

94. Scally A, Durbin R. Revising the human mutation rate: implications for understanding human evolution. Nature Reviews Genetics. 2012; 13: 745–753. https://doi.org/10.1038/nrg3295 PMID: 22965354

95. Narasimhan VM, Rahbari R, Scally A, Wuster A, Mason D, Xue Y, et al. Estimating the human mutation rate from autozygous segments reveals population differences in human mutational processes. Nature Comm. 2017; 8: 303. https://doi.org/10.1038/s41467-017-00323-y PMID: 28827725

96. Fu Q, Hajdinjak M, Moldovan OT, Constantin S, Mallick S, Skoglund P, et al. An early modern human from Romania with a recent Neanderthal ancestor. Nature. 2015; 524: 216–219. https://doi.org/10.1038/nature14558 PMID: 26098372

97. Slon V, Mafessoni F, Vernot B, de Filippo C, Grote S, Viola B, et al. The genome of the offspring of a Neanderthal mother and a Denisovan father. Nature. 2018; 561: 113–116. https://doi.org/10.1038/s41586-018-0455-x PMID: 30135579

98. Henn BM, Steele TE, Weaver TD. Clarifying distinct models of modern human origins in Africa. Curr Opinion Genetics & Develop. 2018; 53:148–156.

99. Durham WH, 1982. Interactions of genetic and cultural evolution: Models and examples. Human Ecol. 1982; 10: 289–323.

100. Laland KN, Odling-Smee J., Feldman MW. Niche construction, biological evolution, and cultural change. Behavioral and Brain Sci. 2000; 23: 131–175.

101. Kendal J, Tehrani JJ, Odling-Smee J. Human niche construction in interdisciplinary focus." Phil. Trans. R. Soc. B. 2011; 366: 785–792. https://doi.org/10.1098/rstb.2010.0306 PMID: 21320894

102. Fogarty L, Creanza N. The niche construction of cultural complexity: interactions between innovations, population size and the environment. Phil. Trans. R. Soc. B 2017; 372: 20160428. https://doi.org/10.1098/rstb.2016.0428 PMID: 29061900

103. Freeman S, Herron JC. Evolutionary analysis. New Jersey: Prentice Hall; 2004.

104. Stringer C. The origin and evolution of *Homo sapiens*. Phil Trans B. 2016; 371: 20150237.

105. Qiu J. The forgotten continent. Nature. 2016; 535:218–220. https://doi.org/10.1038/535218a PMID: 27411595

106. Oppenheimer S. The great arc of dispersal of modern humans: Africa to Australia. Quat Int. 2009; 202: 2–13.

107. Reyes-Centeno H, Ghirotto S, Détroit F, Grimaud-Hervé D, Barbujani G, Harvati K. Genomic and cranial phenotype data support multiple modern human dispersals from Africa and a southern route into Asia. Proc Natl Acad Sci USA. 2014; 111: 7248–7253 https://doi.org/10.1073/pnas.1323666111 PMID: 24753576